Characterization of Homonuclear Diatomic Ions by Semiempirical Morse Potential Energy Curves. 2. The Rare Gas Positive Ions

E. C. M. Chen* and J. G. Dojahn

University of Houston−Clear Lake, Houston, Texas 77058

W. E. Wentworth

Department of Chemistry, University of Houston, Houston, Texas 77024-5641

Received: November 22, 1996; In Final Form: February 21, 1997[⊗]

Morse potential energy curves for the lowest six states of the rare gas positive ion dimers have been calculated on the basis of experimental data. For the ground states, there are sufficient measured data to define the curves completely. For the excited states of all the positive ion dimers except neon, there are sufficient measured data to define the curves. To obtain these curves, new assignments of vibrational progressions in high-resolution photoelectron spectra previously published are made and the vertical ionization potentials obtained. The vertical ionization potentials are used to determine the internuclear distances. The ground state ionic and neutral radii for Ne to Xe are 63, 93, 105, and 123 pm and 112, 152, 168, and 194 pm, respectively. "Virtual" covalent radii for Ne to Xe are 69, 98, 111, and 126 pm. The curves are consistent with the van der Waals radii of Ne to Xe, which are 154, 188, 200, and 218 pm. From the correlation between the Morse parameters of the isoelectronic ions and the new data for the rare gas positive ions, improved Morse potential energy curves for both the halogen negative ion dimers and the rare gas positive ion dimers are obtained.

Introduction

This paper is the second in a series dealing with the determination of semiempirical Morse potential energy curves for homonuclear diatomic ions from diverse experimental data. In part 1, the homonuclear diatomic halogen anions, X_2^-, which are isoelectronic with the homonuclear diatomic rare gas positive ions, Rg_2^+, were discussed.[1] There are now sufficient independent experimental data for the X_2^- and the Rg_2^+ ions to define the Morse potentials of the lowest six electronic states for both.[2,3]

The Rg_2^+ ions are important for reasons that can be found in numerous recent studies of their properties.[2−25] Also, the measured experimental properties of the isoelectronic series complement one another. The bond dissociation energies and frequencies of many of the excited states of the Rg_2^+ ions have been determined from spectroscopic data in contrast to those of the X_2^- ions. Dissociative electron attachment data exist for the X_2^- ions at smaller internuclear distances, while vertical ionization potentials are available for the Rg_2^+ ions at the larger distances. These data help to better define the internuclear distances for both series of diatomic ions.

Currently, more data that can be used to define semiempirical Morse curves exist for the rare gas positive ion dimers than existed for the halogen negative ion dimers 10 years ago when the method for combining data from different sources to obtain complete semiempirical curves was developed.[26] Three to four data points have been reported for each curve or can be obtained from high-resolution photoelectron spectra that have been published for all of the diatomic rare gas positive ions.[2,3] Once the diatomic rare gas positive ion curves have been established, the diatomic halogen negative ion curves can be revised and improved.

Because the neutral rare gas dimers are almost purely dissociative, the dimensionless parameters, k_A, k_B, and k_R, used to combine data from various sources are referenced to a "virtual" rare gas neutral dimer. The "virtual" rare gas neutral dimer is a nonexistent covalently bonded molecule that is used as a basis for comparison with other covalently bonded species that do exist. The properties of this state are obtained by using the values of k_A, k_B, and k_R determined from experimental data for the ground states of the X_2^- and X_2 ions and the experimental data for the ground states of Rg_2^+. The "covalent" radius of the rare gas atom can be taken as one-half of the internuclear distance of the virtual state. In this paper, *Rg2* will refer to this virtual state. The neutral van der Waals molecule will be designated $Rg_{2(vdW)}$.

The Morse potential of the virtual state referenced to zero energy at infinite separation and the parametrized Morse potential for the diatomic positive ions are given by:

$$U(Rg_2) = -2D_{eRg2}\exp(-\beta(r - r_e)) + D_{eRg2}\exp(-2\beta(r - r_e)) \quad (1)$$

$$U(Rg_2^+) = -2k_A D_{eRg2}\exp(-k_B\beta(r - r_e)) + k_R D_{eRg2}\exp(-2k_B\beta(r - r_e)) + E^*_{Rg} \quad (2)$$

where D_{eRg2} represents the spectroscopic bond dissociation energy, r is the internuclear or Rg−Rg separation, $r_e = r$ at the minimum of $U(Rg_2)$, E^*_{Rg} is the energy of the excited state of the rare gas positive ion relative to the ground state, and k_A, k_B, and k_R are dimensionless constants. With ν_e representing the fundamental vibrational frequency, k_{force}, the vibrational force constant, and μ, the reduced mass, β is given by

$$\beta = \nu_e(2\pi^2\mu/D_{eRg2})^{1/2} \quad [\text{where } \nu_e = 1/2\pi(k_{force}/\mu)^{1/2}] \quad (3)$$

Equation 2 is a Morse potential, with the relationships between the properties of the neutral and positive ion being given as

* To whom correspondence should be addressed.

[⊗] Abstract published in *Advance ACS Abstracts,* April 1, 1997.

S1089-5639(96)03895-9 CCC: $14.00

TABLE 1: Experimental Morse Parameters for the Rare Gas Positive Ion Dimers

	D_0 (eV)								r_e (pm)		ν_e (cm^{-1})			
	a	*b*	*c*	*d*	*e*	*f*	*g*	*h*	*a*	*f*	*a*	*b*	*c*	*d*
Ne_2^+														
$^2\Sigma_u^+$	1.341	1.340	>1.291		1.3	1.10	1	1.350	175.3	173	571	570	569	
$^2\Pi_{g,3/2}$	0.154	0.170			0.3				230.4		176			
$^2\Pi_{g,1/2}$	0.080	0.100				0.04			233.0		144			
$^2\Pi_{u,3/2}$	0.058	<0.1				0.04			300.0	307	87			
$^2\Pi_{u,1/2}$	0.105	0.100							286.5	307	113			
$^2\Sigma_g^+$	0.082	0.100				0.04			316.0	307	93			
Ar_2^+														
$^2\Sigma_u^+$	1.384	1.384	1.320	1.361	1.4	1.40	1.230	1.350	245.0	243	320	320	315	
$^2\Pi_{g,3/2}$	0.191	0.200		0.139	0.3				305.9		118	118		
$^2\Pi_{g,1/2}$	0.080	0.080		0.061		0.06			305.4		94	90		
$^2\Pi_{u,3/2}$	0.068	0.065	0.039			0.06			352.1	376	72	70		
$^2\Pi_{u,1/2}$	0.129	0.130	0.077	0.100					345.0	376	90	90		
$^3\Sigma_g^+$	0.073	0.075		0.013		0.06			380.0	376	65	65	59	
Kr_2^+														
$^2\Sigma_u^+$	1.196	1.174	1.174	1.150	1.2	1.20	1.140	1.176	273.1	275	189	190	193	
$^2\Pi_{g,3/2}$	0.220	0.220		0.180	0.3				325.5		77	80		
$^2\Pi_{g,1/2}$	0.059	0.060				0.07			360.3	400	45	45		
$^2\Pi_{u,3/2}$	0.080	0.080	0.047			0.07			364.5	400	54	55	32	
$^2\Pi_{u,1/2}$	0.150	0.150	0.130	0.150					355.4	400	72	70	56	
$^2\Sigma_g^+$	0.078	0.080	0.073	0.028		0.07			410.0	400	43	45		
Xe_2^+														
$^2\Sigma_u^+$	1.010	1.000	0.975	1.030	1.0	1.00	1.020	0.950	316.8	325	128	128	123	133
$^2\Pi_{g,3/2}$	0.194	0.200	0.222	0.202	0.3				368.6		55	55	58	
$^2\Pi_{g,1/2}$	0.056	0.050		0.014		0.08			424.0	436	28	30		
$^2\Pi_{u,3/2}$	0.076	0.080	0.054	0.100		0.08			427.0	436	33	30		
$^2\Pi_{u,1/2}$	0.171	0.170	0.179	0.195					396.7	436	49	50	50	
$^2\Sigma_g^+$	0.104	0.100	0.104	0.025		0.08	0.075		475.0	436	30	30	30	

[a] This work, from combined data. [b] This work, reading from high-resolution photoelectron spectroscopy. [c] References 2 and 3, high-resolution photoelectron spectroscopy. [d] References 7 and 63, photoelectron spectroscopy. [e] Reference 41, scattering. [f] Reference 27, Mulliken's best estimates. [g] References 46−52, photoionization. [h] References 39 and 40, recombination.

before.[1] Once these Morse parameters are defined for the rare gas dimers, the connection to the virtual state is immaterial.

In this paper, a survey of the experimental data and the theoretical values reported in the literature for the rare gas positive ions will be presented. Using photoelectron spectra published in the literature, we have assigned peaks to specific states in order to obtain bond dissociation energies, vibrational frequencies, and vertical ionization potentials. Some of the peak assignments we have made are different from those given previously in the literature. This paper will then discuss the selection of the Morse parameters and will demonstrate the procedure used in the construction of the complete set of Morse curves for each rare gas positive ion dimer.

The internuclear distances are established from the vertical ionization potentials, but consider the absorption spectra, and the order of the states in the Franck−Condon region of the virtual states. Morse potential energy curves for the Rn_2^+ ion are predicted using an extrapolation of the parameters for the Rg_2^+ series based on periodic trends. The semiempirical curves for the diatomic rare gas positive ions and an improved set of curves for the diatomic halogen negative ions are presented. Ionic, covalent, van der Waals, and atomic radii for the halogens and the rare gases will be estimated from these curves and compared with values in the literature.

Survey of Experimental Data in the Literature

It is an especially appropriate time to survey the experimental and theoretical estimates of the spectroscopic properties for the homonuclear diatomic rare gas positive ions. With the recently published high-resolution photoelectron spectra for all of the diatomic rare gas cations, the frequencies, bond dissociation energies, and vertical ionization potentials of all of the states can be measured if the origins and maxima of the bands can be established.[2,3] We have done this and use the results to construct the Morse potentials in this paper.

In Table 1, the experimental Morse parameters for all of the states of the diatomic ions are summarized, with the most recent values from each experimental procedure shown.[2,3,6,13,27−69] The values for D_0, r_e, and ν_e resulting from the combined data which was used to construct the Morse curves presented herein appear in the first column for each parameter in Tables 1 and 2 so that they can easily be compared with the literature values. The values appearing in the second column of Table 1 for D_0 and ν_e are those that we have been obtained from the published high-resolution spectra. Selected theoretically calculated values of the Morse parameters are given in Table 2.[6,12,16−19,70−79] Table 3 presents the auxiliary data that were also considered in constructing the curves.[40−47,53−60] Atomic radii determined from the literature and from these studies are given in Table 4.[80−89]

The experimental values of bond dissociation energies for all the Rg_2^+ ions were summarized by Mulliken in 1970.[27a] Mulliken also estimated the "true" values for these ions as 1.1, 1.4, 1.2, and 1.0 eV for the ground states of Ne_2^+, Ar_2^+, Kr_2^+, and Xe_2^+. With the exception of the Ne_2^+ ion, these are equal to the values obtained from this work, which are listed in column 1 of Table 1. Mulliken proposed that the bond dissociation energies for some of the excited states of these diatomic ions should be equal to the polarization energies at the internuclear distance of the van der Waals dimer. These are listed in Table 1 as estimates from Mulliken and are equal to many of the values determined in this work. Mulliken postulated that the internuclear distances and vibrational frequencies for the Rg_2^+ ions should be proportional to those of the X_2^- ions. The proportionality constant for the internuclear distances is the ratio of the effective nuclear charges and is the same ratio squared for the frequencies. The validity of Mulliken's postulates can now be examined using the current data for the isoelectronic ions.

TABLE 2: Theoretical Morse Parameters for the Rare Gas Positive Ion Dimers

	D_0 (eV)					r_e (pm)					ν_e (cm^{-1})			
	a	*b*	*c*	*d*	*e*	*a*	*b*	*c*	*d*	*e*	*a*	*b*	*c*	*d*
Ne_2^+														
$^2\Sigma_u^+$	1.341	1.310		1.320		175.3	169				571	597		591
$^2\Pi_{g,3/2}$	0.154	0.199		0.09		230.4	214				176	251		
$^2\Pi_{g,1/2}$	0.080	0.137				233.0	215				144	247		
$^2\Pi_{u,3/2}$	0.058	0.054				300.0	254				87	104		
$^2\Pi_{u,1/2}$	0.105	0.078				286.5	250				113	123		
$^2\Sigma_g^+$	0.082	r				316.0	r				93	r		
Ar_2^+														
$^2\Sigma_u^+$	1.384	1.304	1.190	1.340		245.0	243	252	242		320	298	293	309
$^2\Pi_{g,3/2}$	0.191	0.158	0.100	0.22		305.9	302	320	310		118	154	120	100
$^2\Pi_{g,1/2}$	0.080	0.049	r	0.10		305.4	302	r	325		94	147	r	60
$^2\Pi_{u,3/2}$	0.068	0.034	0.010	0.04		352.1	340	410	390		72	54	40	37
$^2\Pi_{u,1/2}$	0.129	0.084	0.040	0.09		345.0	340	360	365		90	88	62	61
$^2\Sigma_g^+$	0.073	r	r	0.01		380.0	r	r	477		65	66	r	26
Kr_2^+														
$^2\Sigma_u^+$	1.196	1.189	1.050	1.01		273.1	275	279	277		189	177	177	165
$^2\Pi_{g,3/2}$	0.220	0.168	0.128	0.17		325.5	348	343	337		77	78	70	87
$^2\Pi_{g,1/2}$	0.059	r	r	r		360.3	r	420	r		45	r	r	r
$^2\Pi_{u,3/2}$	0.080	0.074	0.020	0.03		364.5	385	r	406		54	52	r	36
$^2\Pi_{u,1/2}$	0.150	0.180	0.170	0.11		355.4	364	372	381		72	70	53	51
$^2\Sigma_g^+$	0.078	r	r	r		410.0	r	r	r		43	r	r	r
Xe_2^+														
$^2\Sigma_u^+$	1.010	1.065	0.790	0.890	1.07	316.8	318	327	317	327	128	117	112	113
$^2\Pi_{g,3/2}$	0.194	0.146	0.120	0.19	0.14	368.6	391	r	391	396	55	50	50	64
$^2\Pi_{g,1/2}$	0.056	r	r	0.01	0.01	424.0	r	r	635	528	28	r	r	r
$^2\Pi_{u,3/2}$	0.076	0.038	0.030	0.05	0.07	427.0	400	438	465	436	33	59	30	26
$^2\Pi_{u,1/2}$	0.171	0.206	0.120	0.17	0.21	396.7	397	423	413	404	49	55	47	62
$^2\Sigma_g^+$	0.104	0.025	r	0.03	0.04	475.0	r	551	529	462	30	r	r	21

[a] This work, from combined data. [b] Reference 71, Michels, Hobbs, & Wright. [c] Reference 72, Wadt. [d] (1) Ne ref 6, Bromstrom. (2) Ar ref 19, Gadae. (3) Kr ref 12, Audouard and Spiegelmann. (4) Xe ref 9, Daskalopoulou et al. [e] Xe ref 77, Aramouche et al. Morse fit to calculations from ref 71.

TABLE 3: Auxiliary Data

		E_v (eV)[a]	E_v (eV)[c]	E_{abs} (eV)[a]	E_{abs} (eV)[d]	$r_e\beta^a$		VIP (eV)[a]	VIP (eV)[b]	VIP (eV)[e]	E_{abs} (eV)[a]	E_{abs} (eV)[f]	$r_e\beta^a$	$r_e\beta^g$
$^2\Sigma_u^+$	F_2^-					3.11	Ne_2^+	21.393	21.390				3.66	3.60
$^2\Pi_{g,3/2}$	F_2^-	1.0	1.0	1.60		3.64	Ne_2^+	21.494	21.490		1.703		4.29	4.50
$^2\Pi_{g,1/2}$	F_2^-	1.0	1.0	1.64	1.65	4.23	Ne_2^+	21.530	21.530		1.726	1.75	4.83	4.50
$^2\Pi_{u,3/2}$	F_2^-	3.0	3.0	2.58		3.94	Ne_2^+	21.501	21.500		3.097		4.45	4.50
$^2\Pi_{u,1/2}$	F_2^-	3.1	3.2	2.58		3.65	Ne_2^+	21.556	21.550		3.128	3.10	4.15	4.50
$^2\Sigma_g^+$	F_2^-	6.1	6.0	3.65	3.65	3.93	Ne_2^+	21.575	21.590		4.160	4.20	4.26	4.50
$^2\Sigma_u^+$	Cl_2^-					3.19	Ar_2^+	15.459	15.459	15.548			4.02	4.00
$^2\Pi_{g,3/2}$	Cl_2^-	2.8	2.7	1.58	1.58	4.15	Ar_2^+	15.660	15.660	15.689	1.73	1.70	4.87	4.93
$^2\Pi_{g,1/2}$	Cl_2^-	3.2	2.8	1.62	1.65	5.07	Ar_2^+	15.730	15.730	15.829	1.73	1.73	5.79	4.93
$^2\Pi_{u,3/2}$	Cl_2^-	5.4	5.6	2.28		4.77	Ar_2^+	15.703	15.703	15.734	2.90		5.13	4.93
$^2\Pi_{u,1/2}$	Cl_2^-	5.9	6.0	2.42		4.43	Ar_2^+	15.830	15.830	15.871	3.01	2.90	4.75	4.93
$^2\Sigma_g^+$	Cl_2^-	9.8	9.8	3.40	3.40	4.79	Ar_2^+	15.869	15.870	15.998	4.09	4.00	5.25	4.93
$^2\Sigma_u^+$	Br_2^-					3.50	Kr_2^+	13.690	13.690	13.773			4.15	4.00
$^2\Pi_{g,3/2}$	Br_2^-	0.7	0.7	1.20	1.20	3.96	Kr_2^+	13.890	13.890	13.907	1.25	1.30	4.63	4.80
$^2\Pi_{g,1/2}$	Br_2^-	1.6	1.6	1.61	1.65	4.77	Kr_2^+	13.970	13.970	14.117	1.68	1.70	5.58	4.80
$^2\Pi_{u,3/2}$	Br_2^-	3.8	3.8	1.79		5.22	Kr_2^+	13.951	13.950	14.055	2.14		5.96	4.80
$^2\Pi_{u,1/2}$	Br_2^-	5.4	5.4	2.40		4.89	Kr_2^+	14.571	14.570	14.556	2.86	2.80	5.75	4.80
$^2\Sigma_g^+$	Br_2^-	7.9	8.0	3.22	3.22	5.02	Kr_2^+	14.605	14.605	14.728	3.90	3.90	5.32	4.80
$^2\Sigma_u^+$	I_2^-					4.07	Xe_2^+	11.786	11.785	11.845			4.27	4.00
$^2\Pi_{g,3/2}$	I_2^-	1.2	1.0	1.14	1.14	4.58	Xe_2^+	12.023	12.022	12.021	1.00		4.82	4.75
$^2\Pi_{g,1/2}$	I_2^-	1.8	1.8	1.55	1.55	4.98	Xe_2^+	12.096	12.097	12.198	1.39	1.40	5.25	4.75
$^2\Pi_{u,3/2}$	I_2^-	2.7	2.7	1.65	1.65	4.96	Xe_2^+	12.076	12.076	12.089	1.63	1.65	5.36	4.75
$^2\Pi_{u,1/2}$	I_2^-	3.1	3.0	2.35	2.35	4.53	Xe_2^+	13.310	13.310	13.316	2.63	2.65	4.90	4.75
$^2\Sigma_g^+$	I_2^-	4.1	3.9	3.10	3.11	4.15	Xe_2^+	13.355	13.357	13.518	3.66	3.65	4.65	4.75

[a] This work, from combined data. [b] This work, reading from high-resolution photoelectron spectroscopy. [c] References 1 and 26. [d] References 1, 26, and 88−90. [e] Reference 7. [f] References 53−59. [g] Reference 41.

This landmark paper[27a] by Mulliken initiated an intense study of the diatomic rare gas positive ions and neutral excimers. He presented potential energy curves for all of the states of Xe_2^+ and stated that "these curves are being published in the belief that they can be helpful qualitatively, but it must be emphasized that no general quantitative reliance can be placed on them. This paper is devoted largely to an account of the various considerations used in drawing these curves, so that the reader may judge to what extent reliance can be placed on them. Potential energy curves for the other rare gas positive ions should be similar to those for Xe_2^+". These comments apply appropriately to the Morse curves presented herein, although the curves are now more quantitative since they are defined from experimental data.

In 1978, Herzberg and Huber presented the available spectroscopic data for diatomic molecules and ions but included very limited data on Ne_2^+, Ar_2^+, and Kr_2^+.[28] Preliminary photoelectron spectroscopy data for Xe_2^+ were also presented. In a

1987 review of the thermodynamic properties of ionic clusters, Keesee and Castleman[29] list many values for the bond dissociation energies of the ground state dimer ions. In 1993, the bond dissociation energies of the rare gas positive ions were summarized by Beiske and Maier in a review of the spectroscopy of ionic complexes and clusters.[30]

The effect of clustering in rare gases was first noted by Thompson[31] and was summarized by Loeb.[32] In 1935, the dimeric cations were identified mass spectrometrically by Tuxen,[33] and in 1951, Hornbeck and Molner[34] placed lower limits of 0.7 eV on the bond dissociation energies of all of the Rg_2^+ ions from electron impact threshold data. From mass spectrometric data, this limit was raised in 1963 to about 1 eV for Ar_2^+, Kr_2^+, and Xe_2^+.[35,36] Upper limits of 1.50, 1.64, and 1.15 eV were suggested respectively, on the basis of values that would correspond to the transition to the next higher allowed atomic level that might have served as an appearance potential if the bond dissociation energy were large enough.[37,38] Biondi, Conners, and Frommhold[39,40] determined the bond dissociation energy of Ne_2^+ from the emission spectra from recombination reactions.

In the early 1970s, the bond dissociation energies of the ground state and first excited state of the rare gas positive ion dimers were obtained from scattering experiments[41−47] and photoionization experiments.[37,38,48−52,64−67] Bond dissociation energies of the ground states of the ions and differences between various excited states of Ar_2^+ and Kr_2^+ were obtained from absorption and photodestruction experiments.[53−59]

Since the mid-1970s, photoelectron spectroscopy has been applied to the subject cation dimers, and experimental values for the bond dissociation energies have been obtained.[60−69] In the 1990s, major advances in experimental procedures have led us to the point where values for the bond dissociation energies of all of the states for Ar_2^+, Kr_2^+, and Xe_2^+ can be obtained. In Table 1, the values have been combined from the photoelectron spectroscopy studies of Predeep, Niu, and Shirley[7] and Dehmer, Dehmer, Pratt, and co-workers.[60−63,68,69] The high-resolution photoelectron spectroscopy values reported in 1995 by Lu, Morioka, et al.[2] and Hall et al.[3] are listed separately. These data are reported according to the assignments given in the original articles.

In 1978, Dehmer and Dehmer[62,63] determined the vibrational frequencies for the A $^2\Sigma_u^+$ state of Ar_2^+, Kr_2^+, and Xe_2^+ as 308.9, 188.6, and 132.5 cm^{-1} from photoelectron spectroscopy. The value for Ar_2^+ was confirmed by means of a threshold photoelectron−ion coincidence technique.[14] In 1994, infrared photodissociation spectra of Ar_2^+ gave a vibrational frequency of 117.5 cm^{-1} for the B $^2\Pi_{1/2,g}$ state.[56] More recently, Lu, Morioka, et al.[2] and Hall et al.[3] determined spectroscopic values for the vibrational frequencies for all the ground state and some of the excited state ions using high-resolution photoelectron spectroscopy.

No values for the internuclear distances of the homonuclear diatomic rare gas positive ions from rotational spectra have been reported. The internuclear distances for all of the states are obtained from the measurement of the vertical ionization potentials and energies for maximum absorbance. The ground state values can also be estimated from the sum of the covalent and the ionic radii of the rare gas atoms where available. The internuclear distances for some of the higher excited states are approximately equal to the values of the van der Waals neutral dimers. Atomic radii obtained from these values are given in Table 4.[80−90]

Numerous theoretical calculations of the Morse parameters and complete sets of Morse potential energy curves for the rare gas positive ions can be found in the literature.[6,12,16−19,70−79] The most frequently quoted sets of calculated potential energy curves are those of Michels, Hobbs, and Wright[71] and Wadt.[72] In Table 2, we include the Morse parameters from these two studies. In addition, we include at least one other more recent theoretical calculation, which is discussed below.

For many years, the curves presented by Schneider and Cohen[74] were considered to be the most representative of Ne_2^+. These have been improved upon by the more recent calculations of Brostrom et al.[6] Similarly, the theoretical Morse curves for Ar_2^+ of Woodward, Whitaker, Knowles, and Stace[10] were considered the prototype until a very recent improved set of curves by Gadea and Paidarová were presented.[19] The theoretical calculations of Audouard and Spiegelmann[12] have produced values of D_0, r_e, and ν_e for Kr_2^+. Morse parameters for Xe_2^+ obtained by fitting the data from Michels, Hobbs, and Wright[71] have been presented by Amarouche et al.,[77] and new theoretical calculations have been made by Daskalopoulou et al.[9] As seen in Table 2, these theoretical values of the Morse parameters support the experimental values. The largest discrepancies are for the values of the states that are bound, as opposed to being purely dissociative.

Many theoretical calculations have dealt with only the ground states. The values of the Morse parameters support the experimental values given in Table 1. Theoretical values of the bond dissociation energies for the ground states of Ne_2^+ and Ar_2^+ have been summarized.[16] The values for Ne_2^+ range from 1.3 to 1.4 eV.[6,16,75,76] Many of the theoretical values for the ground state of Ar_2^+ cluster around 1.35 eV, with the value that is closest to the experimental data being that of 1.38 eV.[17] For the ground state of Kr_2^+, theoretical calculations of the bond dissociation energy are between 1.1 and 1.2 eV.[12] The theoretical values of D_0 for Xe_2^+ are approximately 1.0 eV.[3,7,9,71,72,77,78] For the A $^2\Sigma_u^+$ state of Ne_2^+, the values of the internuclear distance range from 169 to 175 pm. The range for the same state in the Ar_2^+ ion is from 243 to 252 pm, in Kr_2^+ from 273 to 279 pm, and in Xe_2^+ from 285 to 322 pm. Except for the excited states of Ne_2^+ and the curves that are considered to be purely dissociative, the theoretical values of the radii and frequencies support the experimental values.

From the above survey, it is clear that until recently very few spectroscopic properties of the rare gas positive ions were available. Previously published potential energy curves for the rare gas dimer cations were plotted by combining experimental data with vibrational frequency and internuclear distance values obtained from theoretical calculations.[41,48,56−58]

Absorption values have been measured experimentally for the B $^2\Pi_{1/2,g}$ and the D $^2\Sigma_g^+$ states of Ar_2^+, Kr_2^+, and Xe_2^+. From this, the absorption values for the respective states of Ne_2^+ can be estimated to be 1.8 and 4.2 eV, respectively. The latter is consistent with a lower limit of 3.54 eV given previously by Lee et al.[53,54] The absorption values for the C $^2\Pi_{1/2,u}$ and C $^2\Pi_{3/2,u}$ states of the diatomic rare gas positive ions can be estimated to fall within the range 2.65−3.00 eV, on the basis of photodestruction data.

Vertical ionization potentials have been experimentally measured for Ar_2^+ by Pradeep, Niu, and Shirley[7] and by Dehmer and Dehmer[62] using photoelectron spectra. However, more precise values of the vertical ionization potentials can be determined from recent high-resolution photoelectron spectra.[2,3] The vertical ionization potentials that we have estimated from these spectra are given in Table 3 along with the values calculated from the Morse potential energy curves.

Differential cross sections for the elastic scattering of Ne^+ on Ne, Ar^+ on Ar, Kr^+ on Kr, and Xe^+ on Xe were measured

TABLE 4: Radii of Atomic Species (pm)

Z	element	r_{vdW}[e]	r_{ion}[e]	r_{closed}[e]	$r_{covalent}$[e]	r_{vdW}[e]	r_{vdW}[a]	r_{met}[b]	r_{ion}[e]	r_{ion}[c]	r_{ion}[d]	r_{closed}[e]	r_{closed}[d]	$r_{covalent}$[e]	$r_{covalent}$[b,c,d]
9	$F^{-0.5}$	170				170									
9	$F^{*-0.5}$	179				179									
9	F^-		119	119					119	119	136	119	136		
9	F				71		155							71	71
9	F^+		62						62						
10	Ne	154		112	69	154	154	131				112	112	69	65
10	$Ne^{+0.5}$	151				151									
10	$Ne^{*+0.5}$	158				158									
10	Ne^+		63						63						
11	Na						227	191							154
11	Na^+		115	115					115	116	95	115	95		
11	Na^-		168						168						
17	$Cl^{-0.5}$	198				198									
17	$Cl^{*-0.5}$	214				214									
17	Cl^-		166	166					166	167	181	166	181		
17	Cl				99		180							99	99
17	Cl^+		90						90						
18	Ar	188		152	98		188					152	154	98	95
18	$Ar^{+0.5}$	188				188									
18	$Ar^{*+0.5}$	176				176									
18	Ar^+		93						93						
19	K						275	235							196
19	K^+		148	148					148	152	133	148	133		
19	K^-		208						208						
35	$Br^{-0.5}$	205				205									
35	$Br^{*-0.5}$	225				225									
35	Br^-		180	180					180	180	195	180	195		
35	Br				114		190							114	114
35	Br^+		104						104						
36	Kr	200		168	111		200	189			169	168	169	111	110
36	$Kr^{+0.5}$	185				185									
36	$Kr^{*+0.5}$	205				205									
36	Kr^+		105						105						
37	Rb							250							209
37	Rb^+		164	164					164	166	148	164	148		
37	Rb^-		231						231						
53	$I^{-0.5}$	236				236									
53	$I^{*-0.5}$	262				262									
53	I^-		206	206					206	206	181	206	216		
53	I				133		204							133	
53	I^+		123						123						
54	Xe	218		194	126		218	218				194	190	126	130
54	$Xe^{+0.5}$	214				214									
54	$Xe^{+0.5}$	237				237									
54	Xe^+		123						123						
55	Cs							272							232
55	Cs^+		181	181					181	181	169	181	169		
55	Cs^-		257						257						

[a] Reference 86. [b] Reference 88. [c] Reference 85. [d] Reference 83. [e] This work.

in 1973 by Mittmann and Weise.[41] The reduced potential is given by eq 4:

$$U_r = -2\exp(-r_e\beta(1 - r/r_e)) + \exp(-2r_e\beta(1 - r/r_e)) \quad (4)$$

These differential cross sections were also considered in the construction of the Morse potential energy curves presented in this paper. Similar values for the reduced exponential parameters, $r_e\beta$, were used, which essentially keep the curves from crossing at smaller internuclear distances.

Assignments and Measurements of Properties from High-Resolution Photoelectron Spectroscopy

The ground state of the rare gas positive ion dimers are designated as A $^2\Sigma_{1/2,u}^+$ [1(1/2u)], and the five excited states are B $^2\Pi_{3/2,g}$ [1(3/2g)], B $^2\Pi_{1/2,g}$ [1(1/2g)], C $^2\Pi_{3/2,u}$ [2(3/2u)], C $^2\Pi_{1/2,u}$ [2(1/2u)], and D $^2\Sigma_g^+$ [2 (1/2g)] in the order of increasing energy at the r_e of the neutral. The strength of the spin orbital coupling increases dramatically with the nuclear charge so that the lighter diatomic rare gases are best described in Hund's case A (the Σ-Π notation), whereas the heavier ones are best described by Hund's rule case C (the alternate notation given in square brackets).[2] For the purposes of a systematic survey, it is convenient to have a uniform set of labels, so we have adopted the Hund's rule case A designation. The identification and reassignment of the different vibrational progressions to the appropriate states is a vital part of this paper. The peaks in the spectrum of Ne_2^+ are not well resolved, so that only approximate assignments can be made. For the other ions, more precise assignments are possible.

The A $^2\Sigma_{1/2,u}^+$ [1(1/2u)] state gives the lowest energy progression of peaks in the spectrum. However, the onset is difficult to determine because the vibrational progression is not the normal Franck−Condon progression. Fortunately, Hall et al. have made these assignments and have reported the spectroscopic properties. Of course, the values depend upon the estimate of the vibrational quantum level and will be different if the onset is different.

For all of the Rg_2^+ ions except Ne_2^+, we identify the highest energy peak observed in the spectrum as the D $^2\Sigma_g^+$ state. For

Ar_2^+, this is in contrast to the assignment given by Hall et al. Hall identified three peaks in the range 15.86−15.90 eV as the C $^2\Pi_{1/2,u}$ state.[3] These peaks are more appropriately assigned to the D $^2\Sigma_g^+$ state. There are, however, three smaller peaks prior to these between 15.82−15.83 eV, which we have assigned to the C $^2\Pi_{1/2,u}$ state.

The B $^2\Pi_{3/2,g}$ [1(3/2g)] states have been previously identified by Predeep, Niu, and Shirley[7] and Dehmer, Dehmer, and coworkers.[60−69] We identify a comparable vibrational progression in the published high-resolution photoelectron spectrum.[2] The B $^2\Pi_{1/2,g}$ state is considered to be purely dissociative, so the peaks are generally located between the two spin orbital atomic ionization potentials. We assign the highest observed peak prior to the lower atomic ionization peak to this state. Hall previously assigned this peak to the C $^2\Pi_{3/2,u}$ state.[3]

The C $^2\Pi_{1/2,u}$ states have been assigned previously by Predeep, Niu, and Shirley[7] and Dehmer, Dehmer, and coworkers.[62,65−67] We find a comparable vibrational progression in the high-resolution photoelectron spectrum for all of the peaks including those of Ar_2^+. As noted previously, the assignment is different from that given by Hall et al. for the C $^2\Pi_{1/2,u}$ state of Ar_2^+. The Morse potentials for the C $^2\Pi_{3/2,u}$ state required the assignment of a new vibrational progression in the photoelectron spectra at about 0.03 eV lower than the sharp peak, which has been now assigned to the B $^2\Pi_{1/2,g}$ state.

The bond dissociation energies of the ions can be estimated from the onset of the vibrational progression and the atomic ionization potentials. In some cases, the onset will be the same as the vertical ionization potential. The separation between peaks in the vibrational progression can be used to obtain the vibrational frequency. In the case of the excited states, this will provide a good estimate of the vibrational frequency as long as the separation between two peaks can be measured.

For the excited states, the vertical ionization potentials can easily be obtained from the high-resolution photoelectron spectra[2,3] if the transitions between the different vibrational progressions can be identified. One need only pick the tallest and most intense peak in the progression to obtain the vertical ionization potential. We have done this and have used these values in the construction of the Morse potential energy curves. The identification of the vertical ionization potential for the ground states is more difficult since the intensity of the peaks does not follow the Franck−Condon pattern. This is a major problem only in the case of the argon dimer. We have selected the peak at 14.46 eV as the vertical ionization peak instead of the one at 14.35 eV, which is very sharp and much more intense. The agreement of the family of curves with all of the other experimental data supports this assignment.

We have estimated the bond dissociation energies and vibrational frequencies for the states that have been assigned above. We report the bond dissociation energy values to two significant figures in Table 1. The vibrational frequency values are reported to ± 5 cm $^{-1}$. No attempt has been made to perform a least squares analysis on the vibrational progressions. The vertical ionization potentials can be used to estimate the internuclear distances if the bond dissociation energies and vibrational frequencies are measured.

Procedures for Calculations

The Morse potentials for the ground states of the rare gas positive ion dimers are calculated by estimating the Morse parameters for the experimental bond dissociation energies and vibrational frequencies given in Table 1. The internuclear distances are estimated from the vertical ionization potentials and agree with the sum of the closed shell and ionic radii of the rare gases. The Morse parameters of the "virtual" state are determined by using the experimental properties of the ground states of the rare gas positive ion dimers and the dimensionless constants, k_A, k_B, and k_R, of the diatomic halogen negative ions.

The curves for the excited states are defined by the experimental values for the bond dissociation energies and vibrational frequencies of the excited states, while the internuclear distances are determined from the vertical ionization potentials (VIPs). The curves are then adjusted to give the experimental absorption maximum. For those excited states for which no absorption maximum has been measured experimentally, values were estimated on the basis of the periodic trend. In addition, the order of the vertical ionization potentials is maintained in both the Franck−Condon regions of the neutral van der Waals dimer. For neon, the order of the vertical ionization potentials is maintained in the Franck−Condon region of the neutral van der Waals dimer. The internuclear distances for the three "nonbonding" states are about equal to the internuclear distance of the neutral van der Waals dimer. In all cases, the vibrational frequencies of the rare gas positive ion dimers are greater than those for the comparative halogen negative ion dimers, and the internuclear distances are all less than those for the corresponding halogen negative ion dimer.

An EXCEL program was set up to plot the Morse curves and to calculate the internuclear distance and the dimensionless parameters, k_A, k_B, and k_R, from the values of D_e and ν_e and the vertical ionization potential. The values of D_e and ν_e can be adjusted to match the experimental maximum energy for the absorption spectra from the ground state. In addition, a QBASIC program was used to calculate and plot distributions for comparison with experimental data.

The internuclear distance can be calculated from the VIP and values of D_e and ν_e by using the following procedure. From the values of D_e and ν_e, the value of k_B can be calculated from the relationship:[1]

$$k_B = \frac{[D_e(Rg_2)]^{1/2}\,\nu_e(Rg_2^+)}{[D_e(Rg_2^+)]^{1/2}\,\nu_e(Rg_2)} \tag{5}$$

The VIP is given by

$$\mathrm{VIP} = \mathrm{IP(Rg)} + U(Rg_2^+) + D_e(Rg_{2(vdW)}) + E^*_{Rg} \tag{6}$$

where $U(Rg_2^+)$ is evaluated at the internuclear distance of the van der Waals neutral dimer. By substituting $y = \exp(-k_B\beta(r(Rg_2) - r_e))$, which is a constant for a given D_e and ν_e, and the relationship[1,26]

$$k_R = k_A^2\{D_e(Rg_2)/D_e(Rg_2^+)\} \tag{7}$$

into the expression for $U(Rg_2^+)$ given by eq 2, a quadratic equation in k_A is obtained:

$$-2k_A y D_e(Rg_2) + k_A^2 y^2\{\{D_e(Rg_2)\}^2/D_e(Rg_2^+)\} - \mathrm{VIP} + \mathrm{IP(Rg)} + D_e(Rg_{2(vdW)}) + E^*_{Rg} \tag{8}$$

This can be solved analytically for k_A so that r_e can be calculated for the values of D_e and ν_e. The use of this calculation for k_A will force the VIP to be equal to the experimental value for other values of D_e and ν_e. These can be chosen to give the experimental energy of maximum absorbance. In practice, the values of D_e and ν_e obtained from the high-resolution photoelectron spectra give reasonable values of the E_{abs} and little adjustment is required, as is seen in Table 1.

The most complete set of published bond dissociation energies and vibrational frequencies are those available for Xe_2^+. We will describe the calculation procedure for Xe_2^+ as an example. The bond dissociation energy and vibrational frequency for the ground state have been measured as 1.01 eV and 127 cm^{-1}, respectively. The vertical ionization potential is equal to 11.786 eV and gives an internuclear distance of 317 pm.

By using the ground state Morse parameters and the values of the dimensionless constants for the ground state of I_2^- (k_A = 1.643, k_B = 0.650, and k_R = 3.937), the Morse parameters of the virtual state can be obtained. The virtual state has an internuclear distance of 252 pm, a bond dissociation energy of 1.47 eV, and a vibrational frequency of 238 cm^{-1}.

Bond dissociation energies for all of the states of Xe_2^+ except for the B $^2\Pi_{1/2,g}$ state have been reported from high-resolution photoelectron spectra.[3] From these same published photoelectron spectra,[2,3] we assign the peak observed at the highest energy below the ionization potential of atomic xenon to the B $^2\Pi_{1/2,g}$ state, instead of the C $^2\Pi_{3/2,u}$ state as previously reported by Hall.[3] For the B $^2\Pi_{1/2,g}$ state, we determine the vertical ionization potential to be 12.096 eV, the bond dissociation energy at 0.05 eV, and the vibrational frequency to be 30 cm^{-1}. In addition, we assign a vibrational progression, which was not previously located, to the C $^2\Pi_{3/2,u}$ state and determine the vertical ionization potential for that state to be 12.076 eV. The bond dissociation energy and vibrational frequency for the C $^2\Pi_{3/2,u}$ state are then determined to be 0.08 eV and 30 cm^{-1}, respectively. The vibrational frequencies of the B $^2\Pi_{3/2,g}$ and C $^2\Pi_{1/2,u}$ states of Xe_2^+ are 58 and 50 cm^{-1}, while a lower limit of 30 cm^{-1} for the D $^2\Sigma_g^+$ state has been established and reported in the literature on the basis of the vibrational spacings.

The Morse parameters were adjusted to give the experimental values of the energies of maximum absorbance 1.39, 1.63, 2.63, and 3.66 eV for the four higher excited states. The distributions for the absorption spectra were calculated. Although the full width at half-maximum for absorption was not used as a defining point of the curves, in many cases it is found to be in reasonable agreement and serves as an additional confirming point. The distribution is significantly affected by temperature, with plots made at higher temperatures (298 K) showing much broader peaks than those seen at lower temperatures (50 K). This was discussed in our previous paper dealing with the homonuclear diatomic halogens anions.[1]

The closed shell radius in the ground state of the rare gas can be obtained by interpolating between the radii of the closed shell halogen negative ion and the alkali metal cation, as suggested by Pauling.[83] For example, in the case of xenon, the radius of I^-, the halogen negative ion, is 206 pm, while that of the isoelectronic Cs^+ is 181 pm. The closed shell radius of Xe is thus 194 pm. Pauling reported a value of 190 pm based on radii of 216 and 169 pm for I^- and Cs^+, respectively. The closed shell radius can also be estimated by obtaining a value of the ionic radius of the rare gas. The ionic radius of Xe^+, 123 pm, is equal to the covalent radius of the isoelectronic halogen, I, of 133 pm divided by the ratio of the effective nuclear charges as calculated by using Slater's rules, or 1.086. The closed shell radius of Xe can then be estimated as the difference between the ground state radius of Xe_2^+ and the ionic radius of Xe^+, which gives 317−123 = 194 pm.

The "covalent" radius of Xe, 126 pm, is one-half of the virtual state covalent radius, 252 pm. This can be compared with an estimate of 130 pm made by Bing-man Fung, based on the internuclear distance of XeF_2,[84] and a value of 126 pm listed by Porterfield.[85] The internuclear distances for the B $^2\Pi_{1/2,g}$, C $^2\Pi_{3/2,u}$, C $^2\Pi_{1/2,u}$, and D $^2\Sigma_g^+$ states of Xe_2^+ are 424, 427, 397, and 475 pm, respectively, and are approximately equal to the internuclear distance of the neutral dimer, 436 pm.[81,82] The consistency of the curves and the use of the vertical ionization potentials to define the curves support the spectroscopic value of 436 pm and give a value of the atomic van der Waals radius of 218 pm. The atomic radius of the $Xe^{+0.5}$ species is estimated at 214 pm by taking half of the internuclear distance of 427 pm. Likewise, the atomic radius for the $Xe^{*+0.5}$ species is estimated as 237 pm or half of 475 pm.

After arriving at a complete set of Morse potential energy curves for Xe_2^+, we reconsidered the curves for I_2^-. The major changes in the Morse parameters for the diatomic halogen anions are in the bond dissociation energies of the excited states and the internuclear distances. In addition to the data for Xe_2^+, we have also considered very recent theoretical and experimental data for these curves presented by Maslen, Faeder, and Parsons.[90] We define the curves by average values of the absorption maxima rather than the matrix values. For example, we use 1.14, 1.55, 1.65, and 2.35 eV obtained from solution values and direct measurements rather than 1.08, 1.53, 1.55, and 2.12 eV based only on matrix isolation values.[91,92] By analogy to Xe_2^+, the I_2^- curves do not cross up to an energy of 7.5 eV.

The atomic radii for the halogens were calculated from the internuclear distances used to construct the Morse potential energy curves in the same manner as described for the rare gases. However, the covalent radius of I is 134 pm or half of the spectroscopic internuclear distance of the neutral. The internuclear distance for the ground state of I_2^-, 340 pm, is determined from the D_e, r_e, and the activation energy for thermal electron attachment. By subtracting the covalent radius from the internuclear distance of the ground state dimer, the ionic radius of I^- is obtained as 340−134 = 206 pm. This is coincidentally equal to the crystal ionic radius. The ionic radii of $I^{-0.5}$ and $I^{*-0.5}$ are estimated as 236 and 262 pm and are both larger than the van der Waals radius of I. The atomic radius of Cs^+ is obtained from the crystalline CsX distances corrected for the coordination number. The radius of Cs^- is estimated from the covalent radius and the internuclear distance for the ground state of Cs_2^-.[89]

In a similar manner, the atomic radius of the halogen positive ion can be obtained from the internuclear distance for the ground state of the halogen positive ion dimers which have been measured experimentally.[28,93−95] For example, the internuclear distance for the homonuclear diatomic positive ion I_2^+ is reported as 258 pm. Using a covalent radius for I of 134 pm, the ionic radius for I^+ is then 124 pm, which is smaller than the covalent radius of I and is about the same as the ionic radius of Xe^+. This is all as expected.

Results and Discussion

Using the calculation procedure described in the previous section, the Morse potential energy curves for the ground states of the rare gas positive ions and for five excited states of the positive ions were calculated. Table 5 gives a summary of the dimensionless constants, k_A, k_B, and k_R, as well as the Morse parameters, D_0, r_e, and ν_e, used to calculate the curves. Also shown in Table 5 are the auxiliary data that have been the most instrumental in the determination of the curves. In the case of the diatomic halogens and their anions, these are the maximum energy for electron attachment and the energy of maximum absorption for the negative ions. For the rare gas positive ion dimers, these include the vertical ionization potentials and the energies of maximum absorption. Atomic radii determined from the literature and from these studies are given in Table 4.[80−89]

TABLE 5: Dimensionless Constants, Morse Parameters, and Defining Data for Potential Energy Curves

		k_A	k_B	k_R	D_0 (eV)	r_e (pm)	ν_e (cm^{-1})	E_v (eV)	E_{abs} (eV)		k_A	k_B	k_R	D_0 (eV)	r_e (pm)	ν_e (cm^{-1})	VIP (eV)	E_{abs} (eV)
neutral		1.000	1.000	1.000	1.600	141.1	917			virtual	1.000	1.000	1.000	1.62	138.0	1160		
$^2\Sigma_u^+$	F_2^-	1.771	0.545	3.856	1.320	189.0	451			Ne_2^+	1.771	0.545	3.856	1.34	175.3	571	21.393	
$^2\Pi_{g,3/2}$	F_2^-	0.534	0.471	2.740	0.164	257.5	140	0.97	1.60	Ne_2^+	0.543	0.486	3.029	0.15	230.4	176	21.494	1.703
$^2\Pi_{g,1/2}$	F_2^-	0.376	0.519	2.432	0.089	262.0	115	0.99	1.64	Ne_2^+	0.376	0.541	2.696	0.08	233.0	144	21.530	1.726
$^2\Pi_{u,3/2}$	F_2^-	0.370	0.394	3.638	0.058	336.0	70	3.00	2.58	Ne_2^+	0.414	0.387	4.575	0.06	300.0	87	21.501	3.097
$^2\Pi_{u,1/2}$	F_2^-	0.517	0.380	4.011	0.105	322.0	90	3.13	2.58	Ne_2^+	0.569	0.379	4.897	0.11	286.5	113	21.556	3.128
$^3\Sigma_g^+$	F_2^-	0.547	0.369	5.856	0.080	357.0	76	6.09	3.65	Ne_2^+	0.571	0.352	6.280	0.08	316.0	93	21.575	4.160
neutral		1.000	1.000	1.000	2.520	199.0	565			virtual	1.000	1.000	1.000	2.55	196.0	728		
$^2\Sigma_u^+$	Cl_2^-	1.208	0.598	2.698	1.366	266.0	248			Ar_2^+	1.208	0.598	2.698	1.38	245.0	320	15.459	
$^2\Pi_{g,3/2}$	Cl_2^-	0.428	0.610	2.374	0.191	339.0	96	2.79	1.58	Ar_2^+	0.445	0.584	2.590	0.19	305.9	118	15.660	1.73
$^2\Pi_{g,1/2}$	Cl_2^-	0.268	0.743	2.197	0.079	340.0	76	3.15	1.62	Ar_2^+	0.278	0.710	2.344	0.08	305.4	94	15.730	1.73
$^2\Pi_{u,3/2}$	Cl_2^-	0.296	0.603	3.137	0.068	394.0	57	5.41	2.28	Ar_2^+	0.352	0.592	4.431	0.07	352.1	72	15.703	2.90
$^2\Pi_{u,1/2}$	Cl_2^-	0.414	0.573	3.521	0.120	385.0	72	5.90	2.42	Ar_2^+	0.477	0.543	4.384	0.13	345.0	90	15.830	3.01
$^2\Sigma_g^+$	Cl_2^-	0.385	0.558	5.005	0.072	428.1	54	9.84	3.40	Ar_2^+	0.406	0.518	5.550	0.07	380.0	65	15.869	4.09
neutral		1.000	1.000	1.000	2.000	228.0	323			virtual	1.000	1.000	1.000	1.99	221.5	405		
$^2\Sigma_u^+$	Br_2^-	1.304	0.604	2.838	1.201	294.0	151			Kr_2^+	1.304	0.604	2.838	1.20	273.1	189	13.690	
$^2\Pi_{g,3/2}$	Br_2^-	0.451	0.590	1.924	0.210	354.0	62	0.70	1.20	Kr_2^+	0.489	0.569	2.140	0.22	325.5	77	13.890	1.25
$^2\Pi_{g,1/2}$	Br_2^-	0.267	0.573	2.002	0.070	408.0	35	1.60	1.61	Kr_2^+	0.276	0.635	2.482	0.06	360.3	45	13.970	1.68
$^2\Pi_{u,3/2}$	Br_2^-	0.355	0.659	3.244	0.076	400.0	42	3.76	1.79	Kr_2^+	0.436	0.660	4.598	0.08	364.5	54	13.951	2.14
$^2\Pi_{u,1/2}$	Br_2^-	0.568	0.607	4.247	0.150	398.0	54	5.37	2.40	Kr_2^+	0.655	0.642	5.593	0.15	355.4	72	14.571	2.86
$^2\Sigma_g^+$	Br_2^-	0.448	0.572	5.255	0.075	448.8	36	7.89	3.22	Kr_2^+	0.485	0.531	5.883	0.08	410.0	43	14.605	3.90
neutral		1.000	1.000	1.000	1.600	267.0	215			virtual	1.000	1.000	1.000	1.47	252.0	238		
$^2\Sigma_u^+$	I_2^-	1.643	0.650	3.937	1.099	340.0	116			Xe_2^+	1.643	0.650	3.937	1.01	316.8	128	11.786	
$^2\Pi_{g,3/2}$	I_2^-	0.585	0.613	2.809	0.194	406.0	46	1.17	1.14	Xe_2^+	0.610	0.630	2.800	0.19	368.6	55	12.023	1.00
$^2\Pi_{g,1/2}$	I_2^-	0.307	0.574	2.639	0.056	470.5	23	1.79	1.55	Xe_2^+	0.327	0.597	2.746	0.06	424.0	28	12.096	1.39
$^2\Pi_{u,3/2}$	I_2^-	0.403	0.577	3.369	0.076	467.0	27	2.66	1.65	Xe_2^+	0.472	0.605	4.243	0.08	427.0	33	12.076	1.63
$^2\Pi_{u,1/2}$	I_2^-	0.610	0.567	3.455	0.171	433.0	40	3.09	2.35	Xe_2^+	0.700	0.595	4.177	0.17	396.7	49	13.310	2.63
$^2\Sigma_g^+$	I_2^-	0.505	0.430	3.864	0.105	524.1	24	4.08	3.10	Xe_2^+	0.633	0.472	5.622	0.10	475.0	30	13.355	3.66
neutral		1.000	1.000	1.000	1.339	297.0	142			virtual	1.000	1.000	1.000	1.33	289.0	153		
$^2\Sigma_u^+$	At_2^-	1.471	0.581	3.002	0.960	369.0	70			Rn_2^+	1.477	0.578	3.029	0.96	348.0	75		
$^2\Pi_{g,3/2}$	At_2^-	0.580	0.580	2.230	0.200	433.0	32		1.04	Rn_2^+	0.611	0.572	2.474	0.20	405.0	34		0.96
$^2\Pi_{g,1/2}$	At_2^-	0.316	0.626	2.185	0.060	478.0	19		1.28	Rn_2^+	0.320	0.611	2.238	0.06	440.0	20		1.21
$^2\Pi_{u,3/2}$	At_2^-	0.550	0.674	3.793	0.105	465.0	27		1.30	Rn_2^+	0.528	0.637	3.506	0.11	430.0	28		1.28
$^2\Pi_{u,1/2}$	At_2^-	0.776	0.661	3.987	0.200	442.0	37		2.30	Rn_2^+	0.701	0.656	3.248	0.20	400.0	39		2.63
$^2\Sigma_g^+$	At_2^-	0.677	0.457	4.504	0.135	540.0	21		3.10	Rn_2^+	0.690	0.433	4.513	0.14	495.0	22		3.59

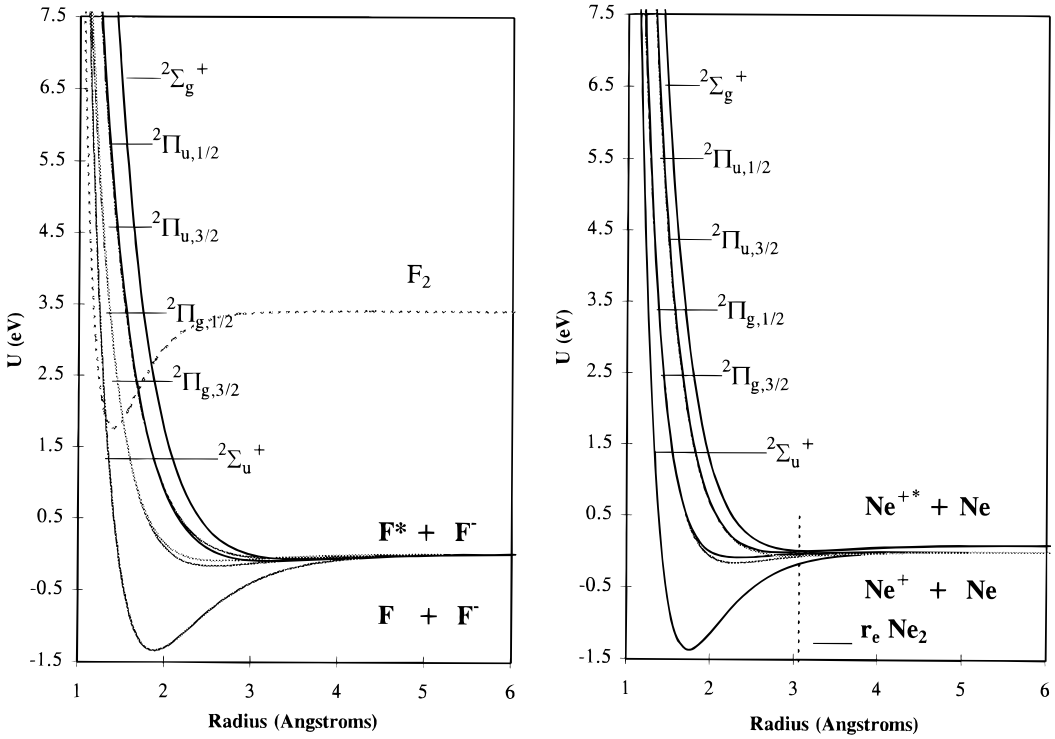

Figure 1. Morse potential energy curves of Ne_2^+, F_2^-, and F_2.

The Morse potentials for all of the Rg_2^+ ions and X_2^- ions are presented in Figures 1−5, including the extrapolations for Rn_2^+ and At_2^-. The diatomic halogen negative ion curves are quite similar to those reported in the first paper of this series. The major difference is that the negative ion curves and the neutral curves do not cross at smaller internuclear distances up to an energy of 7.5 eV.

The Morse potential energy curves presented in Figures 1−4 are the only complete set of semiempirical curves for these species based upon experimental data and the correlation

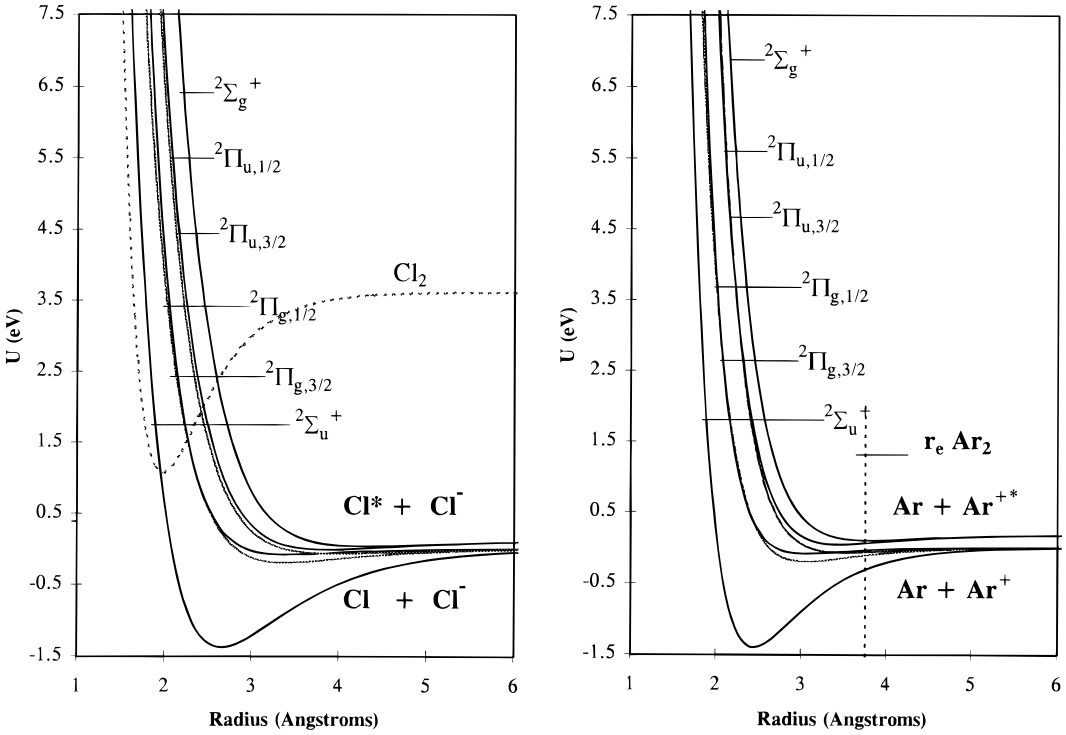

Figure 2. Morse potential energy curves of Ar_2^+, Cl_2^-, and Cl_2.

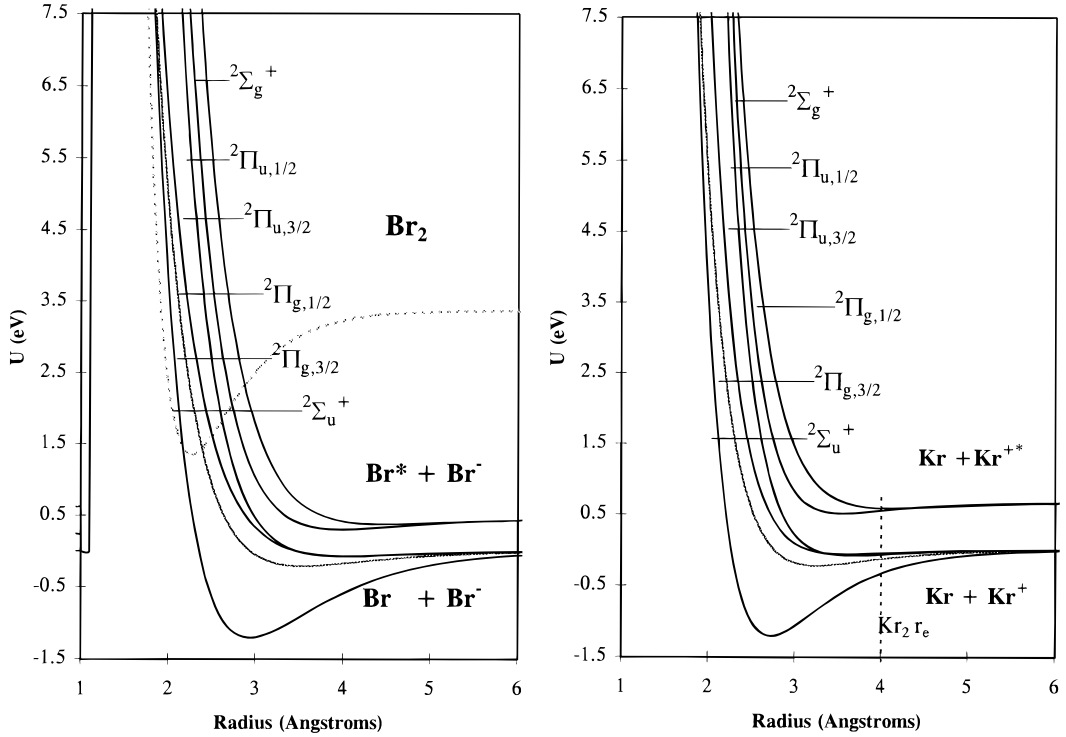

Figure 3. Morse potential energy curves of Kr_2^+, Br_2^-, and Br_2.

between the isoelectronic series. All of the ground state positive ion dimers and the excited state curves for Ar_2^+, Kr_2^+, and Xe_2^+ are defined by more than three experimental data points. The quality of these Morse potentials has been greatly improved. The two factors primarily responsible for this are the publication and analysis of the high-resolution photoelectron spectra for the rare gas positive ions[2,3] and the examination of the isoelectronic series as described herein.

The values of the Morse parameters for the halogen dimer anions and the rare gas dimer cations are plotted as a function of row number in the periodic table in Figures 6−8. The value given first in each plot is for the neutral. The second value represents the ground state of the dimer ion, while the other five values are for the excited states of the ion in the order B $^2\Pi_{3/2,g}$ [1(3/2g)], B $^2\Pi_{1/2,g}$, [1(1/2g)], C $^2\Pi_{3/2,u}$ [2(3/2u)], C $^2\Pi_{1/2,u}$ [2(1/2u)], and D $^2\Sigma_g^+$[2(1/2g)]. This series is then repeated for each subsequent row in the periodic table. In Figure 9, the energy of maximum absorbance for the transitions from the ground state to the excited states is plotted as a function of row number in the periodic table. The first data point is for the transition to the B $^2\Pi_{3/2,g}$ state. The order is then the same as stated above.

The bond dissociation energies of the ground states of the rare gas positive ion dimers and those of the diatomic halogen

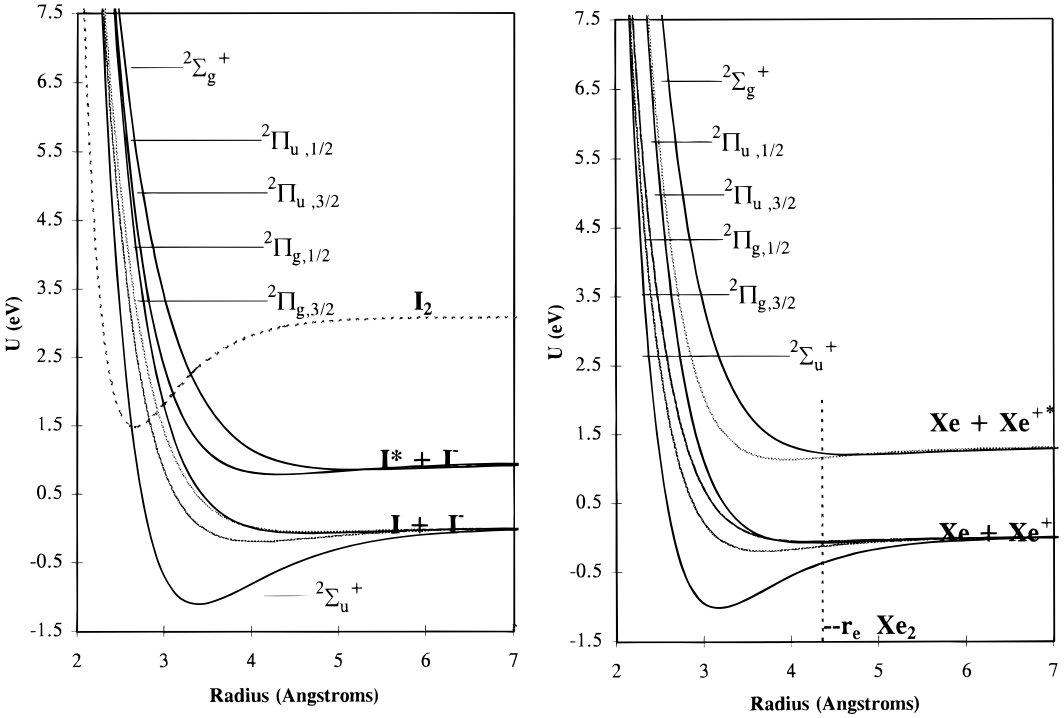

Figure 4. Morse potential energy curves of Xe_2^+, I_2^-, and I_2.

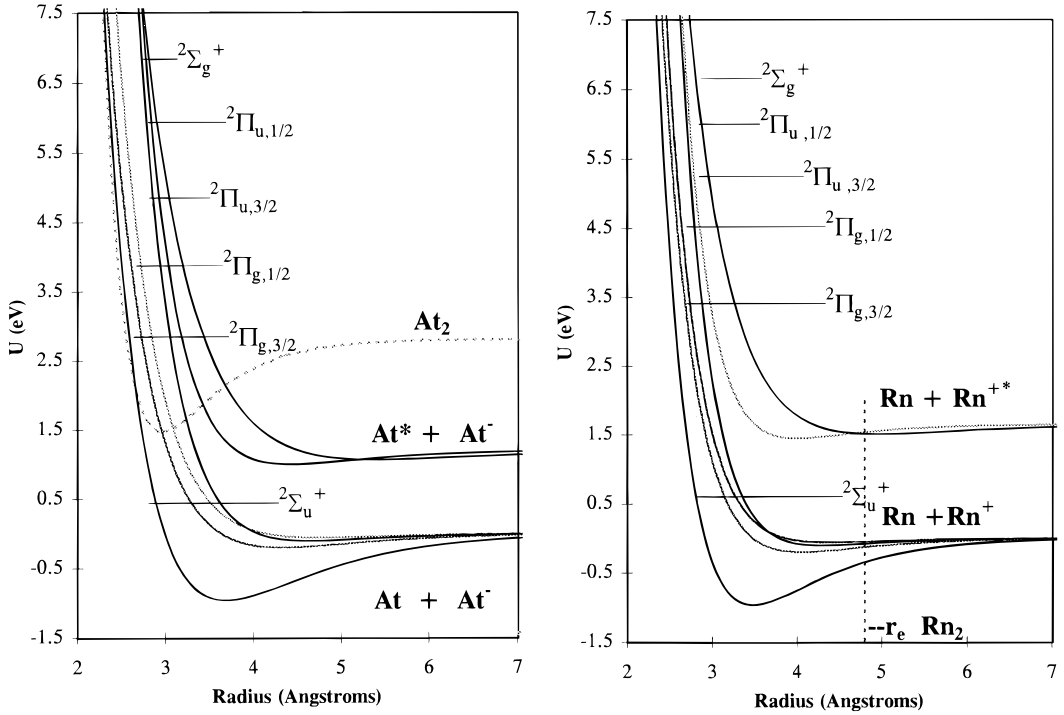

Figure 5. Morse potential energy curves of Rn_2^+, At_2^-, and At_2.

negative ions are measured independently and are equivalent within experimental error. This can be expressed in equation form as $D_e(X_2^-) = (1.00 \pm 0.06)D_e(Rg_2^+)$. With the exception of the excited states of Ne_2^+, all of the bond dissociation energies of the excited states of the rare gas positive ion dimers have been measured spectroscopically. In the case of the halogen negative ion dimers, there are multiple points on the Morse curves to define the bond dissociation energy values. These data include dissociative electron attachment cross sections, vertical electron affinities, and activation energies for thermal electron attachment.[1] The good agreement is not forced and demonstrates the relationship between the bond dissociation energies for these isoelectronic species.

The internuclear distances used to plot the Morse potentials are given in Table 5 and Figure 7. These values are all determined from the vertical ionization potentials and electronic absorption spectra. In addition, the ground state internuclear distances can be obtained from the sum of the covalent and ionic radii. Except for F_2^- and Ne_2^+, the values of the radii for the excited states of X_2^- are proportional to the values for Rg_2^+ with the constant equal to 1.107 ± 0.003. This is equal to the ratio of the Slater effective nuclear charge for Ar to Cl, which is $6.75/6.10 = 1.1065$, as noted by Mulliken. This ratio is a function of the position in the periodic table. From Ne to Xe, the Slater effective nuclear charge ratios are 1.125, 1.1065, 1.0855, and 1.0855. Indeed, these curves can be used as a

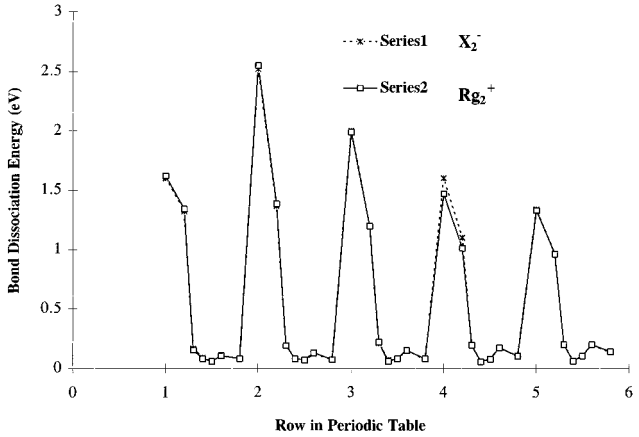

Figure 6. Bond dissociation energies of X_2, X_2^-, Rg_2^+, and the virtual state of Rg_2 as a function of the row in the periodic table.

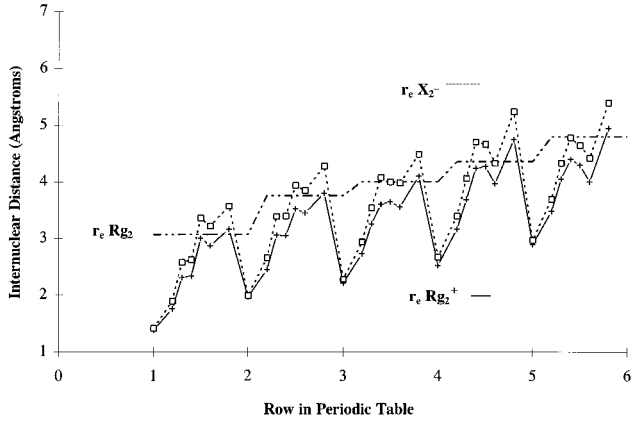

Figure 7. Internuclear distances of X_2, X_2^-, Rg_2^+, and the virtual state of Rg_2 as a function of the row in the periodic table.

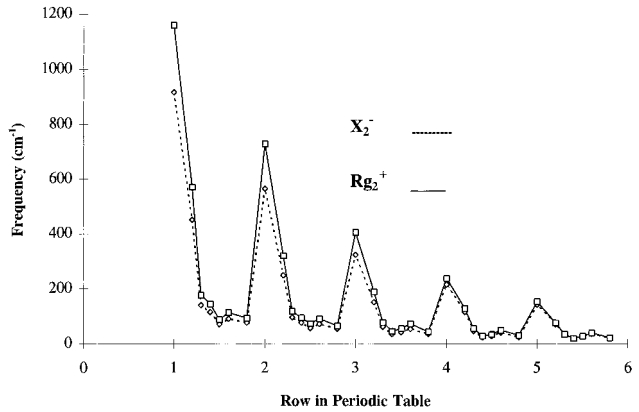

Figure 8. Vibrational frequencies of X_2, X_2^-, Rg_2^+, and the virtual state of Rg_2 as a function of the row in the periodic table.

method of determining this ratio experimentally. For example, the experimental relationship for the excited states is $r(F_2^-) = (1.124 \pm 0.002)r(Ne_2^+)$.

The vibrational frequencies for the ground states of all of the halogen negative ion dimers and the diatomic rare gas positive ions are experimental values. The ground state vibrational frequencies for the diatomic halogen anions were primarily determined by Raman spectroscopy of the matrix-isolated negative ions. The vibrational frequencies determined from high-resolution photoelectron spectra have been obtained for all of the excited states of Ar_2^+, Kr_2^+, and Xe_2^+. For the excited states of the halogen dimer anions, the vibrational frequencies were established by confirmation with other experimental data. It was determined that the vibrational frequencies for the diatomic halogen negative ions are proportional to

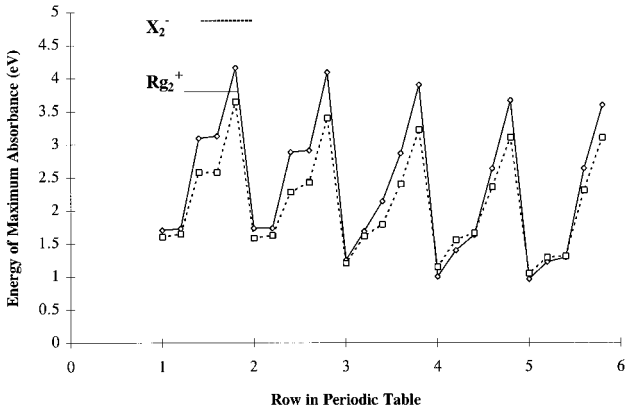

Figure 9. Energy of maximum absorbance from the ground states of X_2^- and Rg_2^+ as a function of the row in the periodic table.

those of the diatomic rare gas positive ions. The proportionality constant is 1.25 ± 0.02, which is approximately equal to the square of the proportionality constant for the radii, $1.107 \times 1.107 = 1.225$. This is also approximately equal to the square of the effective nuclear charge ratio as postulated by Mulliken.

Quality of the Morse Potentials. It is difficult to describe the accuracy of the Morse parameters given in Table 5. The error in the energies for any specific peak in the photoelectron spectra can be estimated and is typically 5 meV for all the diatomic rare gas positive ions except Ne. Hall et al.[3] have cited random errors that range from 2 to 10 meV. However, the bond dissociation energies depend on energy differences and rely on the estimation of the onset. This is especially difficult for the ground state of the rare gas positive ion dimers since the intensities do not follow a normal progression.

The difference between the values for the bond dissociation energies of the ground states of the halogen dimer ions and the diatomic rare gas positive ions range from 0 to 100 meV. Thus for the ground states, the maximum error in the bond dissociation energies is estimated to be 50 meV. The error in the excited state bond dissociation energies is projected to be around 5 meV. Alternatively, the relative error can be estimated to be about 6% of the D_0 value based on the coefficient of variation for the proportionality constant as determined by the comparison of the values for the isoelectronic series.

The random errors in the vibrational frequencies range from 1 to 4 cm^{-1} or 0.25% to 10%, as estimated by Hall et al.[3] For the lower frequencies, or those around 30 cm^{-1}, the error can be as large as 4 cm^{-1}. If a least squares analysis of the vibrational progression were performed, then the error in the vibrational frequency could be established, but this does require that the vibrational quantum number be assigned. When the vibrational frequency is established from the absorption spectra or the vertical ionization potentials and dissociative electron attachment maxima, the error in that quantity must also be considered. For example, the absorption spectra for the diatomic rare gas positive ions in the D $^2\Sigma_g^+$ state are not accurately defined. In the case of the halogen negative ion dimers, the dissociative electron attachment cross sections consist of overlapping combinations which must be deconvoluted and are, hence, not well-defined.[1]

The random errors in the internuclear distances are probably not larger than 10 pm on the basis of the sensitivity of the calculated properties and the scatter in the correlation for the isoelectronic species. In general, the number of significant figures given in Table 5 for the Morse parameters has been chosen to represent an optimistic estimate of the precision of the values so that the curves can be reproduced. The ultimate accuracy of the values is limited by the use of the Morse

function in addition to the precision and accuracy of the experimental data.

The Morse potential can be modified to reflect specific individual data by allowing the dimensionless constants, k_A, k_B, and k_R, to be a function of internuclear distance. For example, the long-range attraction can be modified from the Morse attraction by making the attractive constant, k_A, a function of the internuclear distance in that region. Alternatively, a more detailed analysis of the vibrational progressions in the high-resolution photoelectron spectra could yield more precise potential energy curves than those based on the simple Morse potential.

Atomic Radii. The atomic radii of the rare gases produce a unique challenge for measurement. Before considering this challenge, an acceptable definition of atomic radius must be made. One proposed definition is that the atomic radius is "the closest distance to which it will approach another atom of any size under the circumstances specified".[88] The specified circumstances are in the gas phase, in a single covalent bond, in an ionic lattice, and in a metallic lattice. The term ionic radii has generally referred to the set of radii obtained by assuming additivity of the anion and cation radii to give the internuclear distance in a specific crystal lattice, usually the sodium chloride, 6-coordinate structure. Likewise, the metallic radius is referred to a metallic lattice with a specific coordination number, usually 12. Standard correction factors are available for different coordination numbers.

Originally, we noted that the internuclear distance for the ground state of the halogen negative ions is approximately equal to the sum of the ionic and covalent radii.[26] More recently, we actually used this sum to estimate the internuclear distances of the ground states but failed to emphasize that there were more than three data points to define these curves. In this paper, we return to determining various atomic radii from the internuclear distances of the Morse potentials for the homonuclear diatomic ions. We apply this procedure to the $Rg^{+0.5}$, the $Rg^{*+0.5}$, the $X^{-0.5}$, and the $X^{*-0.5}$ species, as well as to the usual ionic and covalent radii. For purposes of comparison, the procedure is then applied to halogen positive ions and alkali metal negative ions.[28,89,93−98]

The details of the calculations have been presented in the Procedures for Calculations section. Briefly, they consist of using the additivity principle to determine the atomic radius that is least well-defined. For example, in the case of rare gases, the closed shell atomic radius is less well-defined, so it is determined by subtracting the ionic radius of the rare gas from the internuclear distance of the ground state. The ionic radii of the halogens are well-defined, so that the ionic radius of the alkali metal can be determined by subtracting the radius for X^- from the crystal lattice separation. These are presented in Table 4 and compared with literature values for all of the X, Rg, M triads.

Complete experimental values of the covalent, ionic, and closed shell radii have not been reported previously for the rare gases. The internuclear distances of the neutral dimers have been used in this paper to define the vertical ionization potentials so that the Morse potentials support the values that have been determined spectroscopically. Only Xe and Kr form molecules with covalent bonds so that their covalent radii can be measured. However, the procedure for determining covalent radii from the "virtual" state can be used to obtain values for Ne and Ar. Radii for species with a fractional charge can be obtained from the internuclear distances of the excited states. The internuclear distance for the excited states can be divided by 2 to give an apparent van der Waals radius for the fractional positive ions in the ground and excited states. These values bracket the van der Waals radii for the neutral species. The radii of the fractional negative ions of the halogens are comparable except that both the ground and excited state values are larger than the neutral van der Waals radii.

In Figure 10A, the negative ion/van der Waals, closed shell, covalent, and positive ion radii for the X, Rg, and M atoms are plotted. The closed shell radii illustrate the consistency of these values as originally proposed by Pauling.[83] The van der Waals radii for the rare gases are used rather than the negative ion radius. In Figure 10B, the covalent radii of all of the elements are plotted as a function of atomic number. The X, Rg, M triad is shown in larger symbols. A comparison of parts A and B of Figure 10 shows that the positive ion radii are all smaller than the covalent radii, while the negative ion radii are all larger than the covalent radii and the closed shell radii of the rare gases are larger than the corresponding covalent radii. The covalent radii of the rare gases are smaller than the corresponding halogens and are the smallest in a given row, as illustrated in Figure 10B.

Conclusions

The ground and excited states for the homonuclear diatomic rare gas positive ions have been characterized by calculating the Morse potential energy curves from experimental data collected from the literature. These curves are well-defined for both the diatomic rare gas positive ions and the halogen negative ion dimers and can be used to establish reasonable values for the three dimensionless parameters, k_A, k_B, and k_R, used to relate the Morse potentials of the ions to the Morse curves of the neutral or "virtual" molecules. The data sources are high-resolution photoelectron spectra and absorption or photodestruction spectra. Vibrational progressions in the high-resolution photoelectron spectra have been assigned to the six states of all of the rare gas positive ion dimers except Ne_2^+. Some of these are new assignments. Based on these assignments, vibrational frequencies and vertical ionization potentials were estimated. These were combined with the energy of the transitions from the ground state to the neutrals to obtain initial approximations to the Morse potentials. These were refined by considering the scattering data and the order of the states in the Franck−Condon regions of the neutral dimer, and the virtual states have also been used. This set of Morse curves, called the combined curves, is the only complete set of curves obtained from experimental data. We know of no other data to establish a long-range potential at large internuclear distances different from the Morse potential. An improved set of Morse potential energy curves for the negative ion states of the diatomic halogens is obtained by relating these to the curves for the isoelectronic rare gas positive ions.

Using the virtual states as a reference for the rare gas positive ion dimers, the values of the three dimensionless parameters, k_A, k_B, and k_R, for the ground state of the ions are, of course, the same as for the diatomic halogen negative ions. From Table 5, the ranges for these ions are

$$1.771 \geq k_A \geq 1.208$$

$$0.650 \geq k_B \geq 0.548$$

$$3.937 \geq k_R \geq 2.698$$

For the excited states, the ranges for both series of ions are

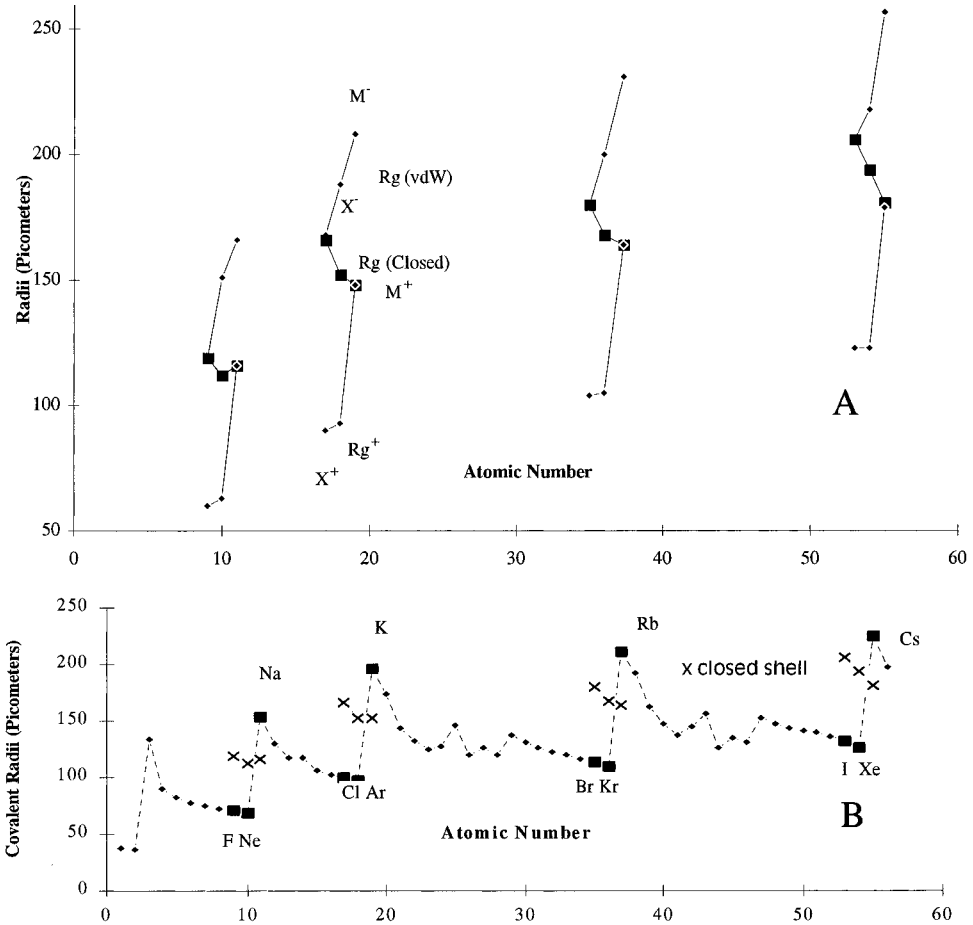

Figure 10. (A) Atomic negative/van der Waals, closed shell, and cationic radii for halogens, rare gases, and alkali metals. (B) Covalent radii for the elements (ref 85) as a function of atomic number (the halogens, rare gases, and alkali metals are in bold symbols).

$$0.658 \geq k_A \geq 0.276$$

$$0.743 \geq k_B \geq 0.352$$

$$6.547 \geq k_R \geq 1.975$$

By combining the ground state Rg_2^+ data with the ground state X_2^- and X_2 data, a "virtual" covalent state of the rare gases can be defined. From these data, "covalent radii" for Ne to Xe are 68, 98, 111, and 126 pm, respectively. The sum of the ionic and atomic radii of the rare gas atoms can be used to conform to the proposed internuclear distance of the ground state. These are generally in good agreement with those in the literature. The ionic and closed shell radii for Ne to Xe are 63, 93, 105, and 123 pm and 112, 152, 168, and 194 pm, respectively. The ionic and covalent radii for F to I are 119, 167, 182, and 206 pm and 71, 99, 114, and 134 pm. "Virtual" covalent radii for Ne to Xe have been determined to be 69, 97, 111, and 126 pm. The Morse curves show a consistency with the van der Waals radii of Ne to Xe, which are 154, 188, 200, and 218 pm, respectively. The corresponding radii for F to I are 155, 180, 190, and 204 pm.

For the excited states, the average of the ratio, $r(X_2^-)/r(Rg_2^+)$ is approximately 1.107 and is equal to the ratio of the Slater effective nuclear charge of Ar to Cl, 6.75/6.10, as noted by Mulliken. The vibrational frequencies of the diatomic rare gas positive ions are approximately proportional to the values for the halogen negative ion dimers, with the proportionality constant approximately equal to 1.25 ± 0.02, which is the square of the ratio of the effective nuclear charges. Alternatively, these Morse potential energy curves can be used to estimate the shielding constants.

Acknowledgment. The authors thank the Robert A. Welch Foundation, Grant E-0095, and the University of Houston At Clear Lake, Grant BC-0022, for support of this work. Initial Morse potential energy curves for the Rg_2^+ ions were based on early literature values obtained by S. Ataalan as part of Master's research at UHCL in 1993.

References and Notes

(1) Dojahn, J. G.; Chen, E. C. M.; Wentworth, W. E. *J. Phys. Chem.* **1996**, *100*, 9649.

(2) Lu. Y.; Morioka, Y.; Matsui, T.; Tanaka, T.; Yoshii, H.; Hall, R. I.; Hayaishi, T.; Ito, K. *J. Chem. Phys*. **1995**, *102*, 1553.

(3) Hall, R. I.; Lu, Y.; Morioka, Y.; Matsui, T.; Tanaka, T.; Yoshii, H.; Hayaishi, T.; Ito, K. *J. Phys. B: At. Mol. Opt. Phys.* **1995**, *28*, 2435.

(4) Lu, Y.; Matsui, T.; Tanaka, K.; Ito, K.; Hayaishi, T.; Morioka, Y. *J. Phys. B* **1992**, *25*, 5101.

(5) Morioka, Y.; Masuda, H.; Lu, Y.; Tanaka, K.; Hayaishi, T. *J. Phys. B* **1992**, *25*, 5343.

(6) Broström, L.; Larsson, M.; Mannervik, S.; Short, R. T.; Sonnek, D. *J. Chem. Soc., Faraday Trans.* **1991**, *87*, 797.

(7) Pradeep, T.; Niu, B.; Shirley, D. A. *J. Chem. Phys.* **1993**, *98*, 5269.

(8) Tonkyn, R. G.; White, M. G. *J. Chem. Phys.* **1991**, *95*, 5582.

(9) Daskalopoulou, M.; Böhmer, H. U.; Peyerimhoff, S. D. *Z. Phys. D* **1990**, *15*, 161.

(10) Woodward, C. A.; Whitaker, B. J.; Knowles, P. J.; Stace, A. J. *J. Chem. Phys.* **1992,** *96*, 3666.

(11) Whitaker, B. J.; Woodward, C. A.; Knowles, P. J.; Stace, A. J. *J. Chem. Phys.*, **1990**, *93*, 376.

(12) Audouard, E.; Spiegelmann, F. *J. Chem. Phys.* **1991**, *94*, 6102.

(13) Green, D. S.; Wallace, S. C. *J. Chem. Phys.* **1994,** *100*, 6129.

(14) Morioka, Y.; Ogawa, M.; Matsumoto, T.; Ito, K.; Tanaka, K.; Hayaishi, T. *J. Phys. At. Mol. Opt. Phys.* **1991**, *24*, 791.

(15) Jones, R. B.; Tran, H. C.; Eden, J. G. *J. Chem. Phys*. **1995**, *102*, 4329
(16) Lopez, G. E. *J. Comput. Chem.* **1995**, *6*, 758.
(17) Pilar de Lara, M,; Villarreal, P.; Delgado-Barrio, G.; Miret-Artes, S.; Buonomo, E.; Gianturco, F. A. *Chem. Phys. Lett*. **1995**, *242*, 336.
(18) Gadea, F. X.; Savrda, J.; Paidarová, I. *Chem. Phys. Lett*. **1994**, *223*, 369.
(19) Gadea, F. X.; Paidarová, I. *Chem. Phys.* **1996**, *209*, 281.
(20) Chen, Y. Z.; May, B. D.; Castleman, A. W., Jr. *Z. Phys. D* **1993**, *25*, 239.
(21) O'Keefe, M.; Brese, N. E. *J. Am. Chem. Soc*. **1991**, *113*, 3226.
(22) Carrington, A.; Pyne, C. H.; Knowles, P. J. *J. Chem. Phys*. **1995**, *102*, 5979.
(23) Lipson, R. H.; Dimov, S. S.; Cai, J. Y.; Wang, P.; Bascal, H. A. *J. Chem. Phys*. **1995**, *102*, 5881.
(24) Mansky, E. J.; Flannery, M. R. *J. Chem. Phys.* **1993**, *99*, 1962.
(25) Ma, N. L.; Li, W.; Ng, C. Y. *J. Chem. Phys*. **1993**, *99*, 3617.
(26) Chen, E. C. M.; Wentworth, W. E. *J. Phys. Chem*. **1985**, *89*, 4099.
(27) a. Mulliken, R. S. *J. Chem. Phys*. **1970,** *52*, 5170. b. Mulliken, R. S. *Radiat. Res*. **1974,** *59*, 357.
(28) Huber, K. P.; Herzberg, G. *Molecular Spectra and Molecular Structure. IV. Constants of Diatomic Molecules;* Van Nostrand-Reinhold: New York, 1979.
(29) Kessee, R. G.; Castleman, A. W. *J. Phys. Chem. Ref. Data* **1986**, *15*, 1011.
(30) Beiske, E. J.; Maier, J. P. *Chem. Rev.* **1993,** *93*, 2603.
(31) Thompson, J. J.; Thompson, G. P. *Conduction of Electricity Through Gases*, Cambridge University Press: Cambridge, 1933.
(32) Loeb, L. B. *Basic Processes of Gaseous Electronics:* University of California Press: Berkeley, 1961.
(33) Tuxen, O. *Z. Phys.* **1936**, *103*, 463.
(34) Hornbeck, J. A.; Molnar, J. P. *Phys. Rev*. **1951**, *84*, 621.
(35) Munson, M. S.; Franklin, J. L.; Field, F. H. *J. Phys. Chem.* **1963**, *67*, 1542.
(36) Melton, C. E.; Hamill, W. H. *J. Chem. Phys*. **1964**, *41*, 1469.
(37) Huffman, R. E.; Katayama, D. H. *J. Chem. Phys*. **1966**, *45*, 138.
(38) Samson, J. A. R.; Cairns, R. B. *J. Opt. Soc. Am*. **1966,** *56*, 1140.
(39) Connor, R. T.; Biondi, M. A. *Phys. Rev.* **1965,** *140*, A778.
(40) Frommhold, L.; Biondi, M. A. *Phys. Rev.* **1969,** *185*, 244.
(41) Mittmann, H. V.; Weise, H. P. *Z. Naturforsch. Teil A* **1974**, *29*, 400.
(42) Vestal, M. L; Blakley C. R.; Futrell, J. H. *Phys. Rev.* **1978**, *A17*, 1337.
(43) Weise, H. P; Mittmann, H. U.; Ding, A.; Henglein, A. *Z. Naturforsch*. **1971**, *A26*, 1112.
(44) Weise, H. P; Mittmann, H. U.; Ding, A.; Henglein, A., *Z. Naturforsch*. **1971**, *A26*, 1122.
(45) Cloney, R. D.; Mason, E. A.; Vanderslice, J. T. *J. Chem. Phys.* **1962,** *36*, 1103.
(46) Lorents, D. C.; Olsen, R. E.; Conklin, G. M. *Chem. Phys. Lett.* **1973**, *20*, 589.
(47) Jones, P. R.; Conklin, G. M.; Lorents, D. C.; Olson, R. E. *Phys. Rev. A* **1974**, *10*, 102.
(48) (a) Ng, C. Y.; Trevor, D. J.; Mahan, B. H.; Lee, Y. T. *J. Chem. Phys.* **1976,** *65*, 4327. (b) Ng, C. Y.; Trevor, D. J.; Mahan, B. H.; Lee, Y. T. *J. Chem. Phys.* **1976,** *66*, 446.
(49) Trevor, D. J.; Pollard, J. E.; Brewer, W. D.; Southworth, S. H.; Truesdale, C. M.; Shirley, A.; Lee, Y. T. *J. Chem. Phys.* **1984**, *80*, 6083.
(50) Trevor, D. J. Ph.D. Thesis, University of California, Berkeley, 1980.
(51) Baker, J. A.; Watts, R. O.; Lee, J. K.; Schafer, T. P.; Lee, Y. T. *J. Chem Phys.* **1974**, *61*, 308.
(52) White, M. G.; Grover, J. R. *J. Chem. Phys*. **1983**, *79*, 4124.
(53) Lee, L. C.; Smith, G. P.; Miller, T. M.; Cosby, P. C. *Phys. Rev. A* **1978**, *17*, 2005.
(54) Lee, L. C.; Smith, G. P. *Phys. Rev. A* **1979**, *19*, 2329
(55) Vanderhoff, J. A. *J. Chem. Phys*. **1978**, *68*, 3311.
(56) Miller, T. M.; Ling, J. H., Saxon, R. P.; Moseley, J. T. *Phys. Rev. A* **1976**, *13*, 2171.
(57) Moseley, J. T.; Saxon, R. P.; Huber, B. A.; Cosby, P. C.; Abouaf, R.; Tadjeddine, M. *J. Chem. Phys.* **1977**, *67*, 1659.
(58) Abouaf, R.; Huber, B. A.; Cosby, P. C.; Saxon, R. P.; Moseley, J. T. *J. Chem. Phys.* **1978,** *68*, 2406.
(59) Geohegen, D. B.; Eden, J. G. *J. Chem. Phys*. **1988**, *89*, 3410.
(60) Pratt, S. T.; Dehmer, J. L.; Dehmer, P. M. *Chem. Phys. Lett.* **1990**, *165*, 131.
(61) Dehmer, P. M.; Pratt, S. T. VUV Spectroscopy of Rare Gas Van der Waals Dimers. In *Photophysics and Photochemistry in the Vacuum Ultraviolet;* McGlynn, S. P., Findlay, G. L., Huebner, R. H., Eds.; Reidel: Dordrecht, 1985; p 467.
(62) Dehmer, P. M.; Dehmer, J. L. *J. Chem. Phys.* **1978**, *69*, 125.
(63) Dehmer, P. M.; Dehmer, J. L. *J. Chem. Phys.* **1978**, *68*, 3462.
(64) Pratt, S. T.; Dehmer, P. M. *Chem. Phys. Lett.* **1982**, *87*, 533.
(65) Dehmer, P. M.; Pratt, S. T. *J. Chem Phys.* **1982**, *76*, 843.
(66) Dehmer, P. M.; Poliakoff, E. D. *Chem. Phys. Lett*. **1981**, *77*, 326.
(67) Dehmer, P. M. *J. Chem. Phys.* **1982,** *76*, 1263.
(68) Dehmer, P. M.; Pratt, S. T.; Dehmer, J. L. *J. Phys. Chem.* **1987**, *91*, 2593.
(69) Dehmer, P. M.; Pratt, S. T. *J. Chem. Phys.* **1988**, *88*, 4139.
(70) Stevens, W. J.; Gardner, M.; Karo, A.; Julienne, P. *J. Chem. Phys.* **1977**, *67*, 2861.
(71) Michels, H. H.; Hobbs, R. H.; Wright, L. A. *J. Chem. Phys.* **1978**, *69*, 5151.
(72) Wadt, W. R. *J. Chem. Phys.* **1978**, *68*, 402.
(73) Duffy, L. M.; Feinberg, T. N.; Baer, T. *J. Chem. Phys.* **1994**, *101*, 2793.
(74) (a) Cohen, J. S.; Schneider, B. *J. Chem. Phys*. **1974**, *61*, 3230. (b) Schneider, B.; Cohen, J. S. *J. Chem. Phys*. **1974**, *61*, 3240.
(75) Gilbert, T. L.; Wahl, A. C. *J. Chem. Phys*. **1971**, *55*, 5247.
(76) Gill, P. M. W.; Radom, L. *J. Am. Chem. Soc*. **1988**, *110*, 4931.
(77) Amarouche, M.; Durand, G.; Malrieu, J. P. *J. Chem. Phys*. **1987**, *88*, 1010.
(78) Ermler, W. C.; Lee, Y. S.; Pitzer, K. S.; Winter, N. W. *J. Chem. Phys*. **1978**, *69*, 976.
(79) Brunetti, B.; Cambi, R.; Pirani, F.; Vecchiocattivi, F.; Tomassini, M. *Chem. Phys*. **1979**, *42*, 397.
(80) Tanaka, Y.; Yoshino, K. *Chem. Phys. Lett*. **1972**, *57*, 2964.
(81) Tanaka, Y.; Yoshino, K.; Freeman, D. E. *J. Chem. Phys.* **1973**, *59*, 5160.
(82) Tanaka, Y.; Yoshino, K. *J. Chem. Phys.* **1970**, *53*, 2012.
(83) Pauling, L. *The Nature of the Chemical Bond*, 3rd. ed.; Cornell University Press: Ithaca, NY, 1960.
(84) Fung, B.-M. *J. Chem. Phys*. **1965**, *69*, 596.
(85) Porterfield, W. W. *Inorganic Chemistry*, 2nd ed.; Academic Press: San Diego, CA, 1994.
(86) Huheey, J. E. *Inorganic Chemistry*, 2nd ed.; Harper and Row: New York, 1978.
(87) Sanderson, R. T. *Polar Covalence;* Academic Press: San Diego, CA, 1983.
(88) Dean, J. A., Ed. *Lange's Handbook of Chemistry*, 13th ed.; McGraw Hill: New York, 1985.
(89) Dojahn, J. G. Master of Science Thesis, University of Houston−Clear Lake, 1994.
(90) Maslen, P. E.; Faeder, J.; Parson, R. *Chem. Phys. Lett.*, accepted for publication.
(91) Shida, T.; Takahashi, Y.; Hatano, H. *Chem. Phys. Lett.* **1975**, *33*, 491.
(92) Papanikolas, J. M.; Gord, J. R.; Levinger, N. E.; Ray, D.; Vorsa, V.; Lineberger, W. C. *J. Phys. Chem.* **1991**, *95*, 8028.
(93) Cartwright, D. C.; Hay, P. J. *Chem. Phys*. **1987**, *114*, 305.
(94) Harris, T.; Eland, J. D. H.; Tuckett, R. P. *J. Mol. Spectrosc*. **1993**, *98*, 269.
(95) Mason, S. M.; Tuckett, R. P. *Chem, Phys. Lett*. **1989**, *160*, 575.